Observation of Transverse Polarization Asymmetries of Charged Pion Pairs in e^{+}e^{-} Annihilation near sqrt[s]=10.58 GeV

A. Vossen *et al.* (Belle Collaboration)

Observation of transverse polarization asymmetries of charged pion pairs in e^+e^- annihilation near $\sqrt{s} = 10.58$ GeV.

A. Vossen,[9,50] R. Seidl,[34] I. Adachi,[8] H. Aihara,[43] T. Aushev,[20,13] V. Balagura,[13] W. Bartel,[3] M. Bischofberger,[24] A. Bondar,[1,31] M. Bračko,[22,14] T. E. Browder,[7] M.-C. Chang,[2] A. Chen,[25] P. Chen,[27] B. G. Cheon,[6] K. Cho,[17] Y. Choi,[38] S. Eidelman,[1,31] M. Feindt,[16] V. Gaur,[40] N. Gabyshev,[1,31] A. Garmash,[1,31] B. Golob,[21,14] M. Grosse Perdekamp,[9,34] J. Haba,[8] K. Hayasaka,[23] Y. Horii,[42] Y. Hoshi,[41] W.-S. Hou,[27] H. J. Hyun,[19] K. Inami,[23] A. Ishikawa,[35] M. Iwabuchi,[49] Y. Iwasaki,[8] T. Iwashita,[24] N. J. Joshi,[40] H. Kichimi,[8] H. O. Kim,[19] M. J. Kim,[19] B. R. Ko,[18] T. Kumita,[45] J. S. Lange,[4] M. J. Lee,[37] S.-H. Lee,[18] M. Leitgab,[9,34] Y. Li,[47] C. Liu,[36] D. Liventsev,[13] R. Louvot,[20] S. McOnie,[39] H. Miyata,[29] Y. Miyazaki,[23] R. Mizuk,[13] G. B. Mohanty,[40] E. Nakano,[32] S. Nishida,[8] O. Nitoh,[46] A. Ogawa,[34] T. Ohshima,[23] S. Okuno,[15] G. Pakhlova,[13] H. Park,[19] H. K. Park,[19] M. Petrič,[14] L. E. Piilonen,[47] S. Ryu,[37] H. Sahoo,[7] Y. Sakai,[8] O. Schneider,[20] C. Schwanda,[11] O. Seon,[23] M. Shapkin,[12] V. Shebalin,[1,31] T.-A. Shibata,[33,44] J.-G. Shiu,[27] P. Smerkol,[14] Y.-S. Sohn,[49] E. Solovieva,[13] S. Stanič,[30] M. Starič,[14] M. Sumihama,[33,5] T. Sumiyoshi,[45] Y. Teramoto,[32] M. Uchida,[33,44] S. Uehara,[8] T. Uglov,[13] Y. Unno,[6] S. Uno,[8] G. Varner,[7] A. Vinokurova,[1,31] C. H. Wang,[26] M.-Z. Wang,[27] P. Wang,[10] Y. Watanabe,[15] E. Won,[18] B. D. Yabsley,[39] Y. Yamashita,[28] V. Zhilich,[1,31] P. Zhou,[48] and V. Zhulanov[1,31]

(The Belle Collaboration)

[1]Budker Institute of Nuclear Physics, Novosibirsk
[2]Department of Physics, Fu Jen Catholic University, Taipei
[3]Deutsches Elektronen–Synchrotron, Hamburg
[4]Justus-Liebig-Universität Gießen, Gießen
[5]Gifu University, Gifu
[6]Hanyang University, Seoul
[7]University of Hawaii, Honolulu, Hawaii 96822
[8]High Energy Accelerator Research Organization (KEK), Tsukuba
[9]University of Illinois at Urbana-Champaign, Urbana, Illinois 61801
[10]Institute of High Energy Physics, Chinese Academy of Sciences, Beijing
[11]Institute of High Energy Physics, Vienna
[12]Institute of High Energy Physics, Protvino
[13]Institute for Theoretical and Experimental Physics, Moscow
[14]J. Stefan Institute, Ljubljana
[15]Kanagawa University, Yokohama
[16]Institut für Experimentelle Kernphysik, Karlsruher Institut für Technologie, Karlsruhe
[17]Korea Institute of Science and Technology Information, Daejeon
[18]Korea University, Seoul
[19]Kyungpook National University, Taegu
[20]École Polytechnique Fédérale de Lausanne (EPFL), Lausanne
[21]Faculty of Mathematics and Physics, University of Ljubljana, Ljubljana
[22]University of Maribor, Maribor
[23]Nagoya University, Nagoya
[24]Nara Women's University, Nara
[25]National Central University, Chung-li
[26]National United University, Miao Li
[27]Department of Physics, National Taiwan University, Taipei
[28]Nippon Dental University, Niigata
[29]Niigata University, Niigata
[30]University of Nova Gorica, Nova Gorica
[31]Novosibirsk State University, Novosibirsk
[32]Osaka City University, Osaka
[33]Research Center for Nuclear Physics, Osaka
[34]RIKEN BNL Research Center, Upton, New York 11973
[35]Saga University, Saga
[36]University of Science and Technology of China, Hefei
[37]Seoul National University, Seoul
[38]Sungkyunkwan University, Suwon

^{39} *School of Physics, University of Sydney, NSW 2006*
^{40} *Tata Institute of Fundamental Research, Mumbai*
^{41} *Tohoku Gakuin University, Tagajo*
^{42} *Tohoku University, Sendai*
^{43} *Department of Physics, University of Tokyo, Tokyo*
^{44} *Tokyo Institute of Technology, Tokyo*
^{45} *Tokyo Metropolitan University, Tokyo*
^{46} *Tokyo University of Agriculture and Technology, Tokyo*
^{47} *CNP, Virginia Polytechnic Institute and State University, Blacksburg, Virginia 24061*
^{48} *Wayne State University, Detroit, Michigan 48202*
^{49} *Yonsei University, Seoul*
^{50} *Indiana University, Bloomington, Indiana 47408*

The interference fragmentation function translates the fragmentation of a quark with a transverse projection of the spin into an azimuthal asymmetry of two final-state hadrons. In e^+e^- annihilation the product of two interference fragmentation functions is measured. We report nonzero asymmetries for pairs of charge-ordered $\pi^+\pi^-$ pairs, which indicate a significant interference fragmentation function in this channel. The results are obtained from a 672 fb^{-1} data sample that contains 711×10^6 $\pi^+\pi^-$ pairs and was collected at and near the $\Upsilon(4S)$ resonance, with the Belle detector at the KEKB asymmetric-energy e^+e^- collider.

The transverse spin structure of the nucleon is only poorly understood as its extraction requires the knowledge of spin-dependent fragmentation functions. Here we report the observation of transverse asymmetries of charged pion pairs in e^+e^- annihilation near a center of mass energy of 10.58 GeV. These results can be used to extract the interference fragmentation function (IFF).

The IFF, first suggested by Collins [1], is sensitive to the transverse polarization of the fragmenting quark and thus can be used as a quark polarimeter. The previous measurement of the Collins fragmentation function [2, 3] with the Belle detector allowed the first global analysis of transversity [4] to be performed using data from HERMES [5] and COMPASS [6]. Knowledge of the IFF will allow complementary access to transversity and a comparison to the Lattice QCD calculations [7]. Moreover, by detecting a second hadron, the sensitivity to the quark spin survives integration over transverse momenta. Thus, unlike the Collins effect, collinear models can be used for factorization and the QCD evolution of the fragmentation function is known [8]. Like the Collins function, the IFF is chiral-odd and can be used to extract transversity from asymmetries measured in polarized semi-inclusive deep inelastic scattering (SIDIS) [9, 10] or proton-proton scattering [11].

The quantity sensitive to the transverse polarization of quarks is a cosine modulation of the azimuthal angle ϕ of the plane spanned by the momenta of the two hadrons h_1, h_2 around the fragmenting quark direction with respect to the transverse quark spin. However, while the quark spin is unknown in unpolarized $e^+ e^-$ scattering, the two primordial quarks appear in two back-to-back jets. The kinematics of the process is shown in Fig. 1. Thus, instead of measuring the azimuthal angle between the spin vector and the vector $\mathbf{R} = \mathbf{P}_{h1} - \mathbf{P}_{h2}$ describing

the two-hadron-plane, one measures an azimuthal correlation of two hadron pairs detected in opposite hemispheres $\alpha = 1, 2$. The angles ϕ_1 and ϕ_2 are defined in the center-of-mass system (CMS) between $\mathbf{R}_\alpha$ and the event plane spanned by the electron-positron axis $\hat{\mathbf{z}}$ and the thrust axis $\hat{\mathbf{n}}$ [12]. They can be expressed in terms of measured quantities as:

$$
\begin{aligned}
\phi_{\{1,2\}} &= \text{sgn} \left[\hat{\mathbf{n}} \cdot (\hat{\mathbf{z}} \times \hat{\mathbf{n}} \times (\hat{\mathbf{n}} \times \mathbf{R}_{1,2})) \right] \\
&\times \ \arccos \left(\frac{\hat{\mathbf{z}} \times \hat{\mathbf{n}}}{|\hat{\mathbf{z}} \times \hat{\mathbf{n}}|} \cdot \frac{\hat{\mathbf{n}} \times \mathbf{R}_{1,2}}{|\hat{\mathbf{n}} \times \mathbf{R}_{1,2}|} \right) \quad .
\end{aligned}
\tag{1}
$$

As in the Collins analysis, a second method can be applied, which does not directly depend on the thrust axis to calculate the angles, but defines the reference axis via the momentum of the second hadron pair and corresponding angles ϕ_{1R} and ϕ_{2R}. Using either set of angles, ϕ_1, ϕ_2 or ϕ_{1R}, ϕ_{2R}, one can obtain a $\cos(\phi_{1(R)} + \phi_{2(R)})$ modulation proportional to the interference fragmentation functions normalized by the corresponding unpolarized di-hadron fragmentation functions. The amplitude of this modulation in e^+e^- annihilation is according to Boer [13]:

$$
\begin{aligned}
a_{12R}(z_1, z_2, m_1^2, m_2^2) &\propto \frac{1}{2} \frac{\sin^2\theta}{1 + \cos^2\theta} \cdot \\
\frac{\sum_{q,\overline{q}} \ e_q^2 \ z_1^2 z_2^2 \ H_1^{\sphericalangle \, q}(z_1, m_1^2) \ H_1^{\sphericalangle \, \overline{q}}(z_2, m_2^2)}{\sum_{q,\overline{q}} \ e_q^2 \ z_1^2 z_2^2 \ D_1^q(z_1, m_1^2) \ D_1^{\overline{q}}(z_2, m_2^2)} &,
\end{aligned}
\tag{2}
$$

and a similar formula for the $\cos(\phi_1 + \phi_2)$ modulation amplitude a_{12}. The interference fragmentation function $H_1^{\sphericalangle, q}$ of a quark q (and charge e_q) , and its polarization-independent counterpart D_1^q, depend on the fractional energy $z_\alpha \overset{CMS}{=} 2E_\alpha/\sqrt{s}$ of the hadron pair in hemisphere α and on its invariant mass m_α. The CMS energy is

denoted by $\sqrt{s}$ and the polar angle θ is defined between the beam axis and the reference axis in the CMS. As dependence on the polar angle is a clear indication of initial transverse quark polarization, this dependence was studied.
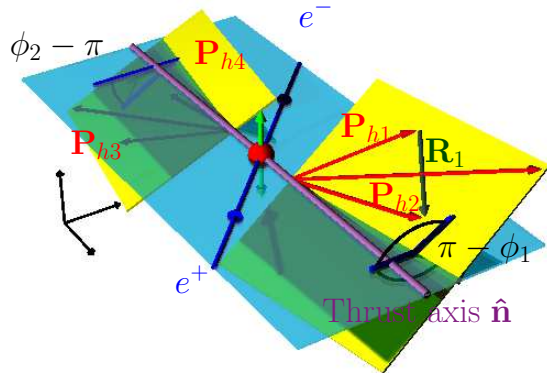

FIG. 1: Azimuthal angle definitions for ϕ_1 and ϕ_2 as defined relative to the thrust axis in the CMS.

Collins and Ladinsky[14] used the linear sigma model to make the first predictions for π-π correlations. Another approach makes use of a partial wave analysis to arrive at predictions for $H_1^{\sphericalangle}$, which receives essential contributions from the interference of meson pairs (pions and kaons) in relative S- and P-wave states [15–17]. A strong dependence on the invariant mass of the hadron pair is predicted. Predictions for the IFF can be found in papers by Jaffe, Jin and Tang [18] and from references [19, 20], with the latter being recently extended to e^+e^- annihilation [21] at Belle energies. Jaffe and collaborators estimate the final-state interactions of the meson pairs from meson-meson phase shift data in [22], where it is observed that S- and P-wave production channels interfere strongly in the mass region around the ρ, the K^* and the ϕ meson resonances, and give rise to a sign change of the IFF.

This analysis is based on a 672 fb^{-1} data sample collected with the Belle detector at the KEKB asymmetric-energy e^+e^- (3.5 on 8 GeV) collider [23] operating at the $\Upsilon(4S)$ resonance and 60 MeV below. The Belle detector is a large-solid-angle magnetic spectrometer that consists of a silicon vertex detector (SVD), a 50-layer central drift chamber (CDC), an array of aerogel threshold Cherenkov counters (ACC), a barrel-like arrangement of time-of-flight scintillation counters (TOF), and an electromagnetic calorimeter (ECL) comprised of CsI(Tl) crystals located inside a superconducting solenoid coil that provides a 1.5 T magnetic field. An iron flux-return yoke located outside of the coil is instrumented to detect K_L^0 mesons and to identify muons (KLM). The detector is described in detail elsewhere [24].

The most important selection criterion is the event shape variable thrust, T, the maximum of which defines the thrust axis $\hat{\mathbf{n}}$: $T \stackrel{max}{=} \frac{\sum_h |\mathbf{P}_\mathbf{h}^{\mathrm{CMS}} \cdot \hat{\mathbf{n}}|}{\sum_h |\mathbf{P}_\mathbf{h}^{\mathrm{CMS}}|}$. The sum extends over all detected particles, and P_h^{CMS} denotes their momenta in the CMS. The cosine of the deviation from reconstructed thrust axis and generated quark-antiquark pair axis for light quarks is 0.990 with an RMS of 0.015, as obtained from the simulated sample of events using the PYTHIA [27] event generator and a GEANT [28] detector simulation. This value is compatible with those cited earlier in the Collins analysis [2]. Since the two pairs of hadrons should appear in a two-jet topology, events are selected with a thrust value larger than 0.8. The contamination from B decays in this event sample is around 2% [3]. As the hadron pairs are sampled only in the barrel region of the detector, one has to ensure that for those pairs all possible azimuthal angles around the thrust axis lie also within this acceptance. For this purpose only events with a thrust axis pointing into the central detector are considered with the z component of the thrust unit vector $|\hat{\mathbf{n}}_z| < 0.75$. In order to obtain a reliable thrust axis and to reduce the contribution from $e^+e^- \rightarrow \tau^+\tau^-$ events, the reconstructed energy of an event is required to be above 7 GeV. Tracks are required to lie in the central part of the detector acceptance corresponding to $-0.6 < \cos(\theta_{LAB}) < 0.9$, where θ_{LAB} is the polar angle in the laboratory frame. This corresponds to a nearly symmetric track selection in the CMS frame, with the polar angle range $-0.79 < \cos(\theta_{CMS}) < 0.74$. All tracks are required to originate from a region around the reconstructed interaction point, which is defined by the requirements $dr < 2$ cm and $|dz| < 4$ cm, where dr and dz are the distance of closest approach to the interaction point in the plane perpendicular to the beam direction and along the direction of the beams. Pions were selected among the reconstructed charged tracks by vetoing identified muons, electrons and protons, and requiring a kaon - pion particle identification likelihood to be larger than 0.7 [26]. With these requirements the fraction of fake pions in the selected sample is between 2.7 and 3.3%. The overall fraction of misidentified pions, obtained from simulated data, is added as a relative systematic uncertainty of the final measured asymmetries and is correlated between the bins defined below. All pions are required to have a minimal fractional energy $z = \frac{2E_h}{\sqrt{s}} > 0.1$. The fractional energy z_α of each pion pair is thus at least 0.2.

In addition to θ_{LAB}, other polar angles in this analysis are the polar angle of the thrust axis in the CMS $\theta_t = \mathrm{acos}(\hat{\mathbf{n}}_z)$ and the decay angles of a hadron pair in their respective center-of-mass systems $\theta_{1d,2d}$ defined with respect to the first (i.e., positive) hadron. The lowest-order interference fragmentation term has a $\sin\theta_d$ distribution.

Any combination of two charged pions with opposite

charge is combined in a pair if the two hadrons are in the same hemisphere. For the analysis we select two pion pairs belonging to opposite hemispheres. In addition, the requirement of an opening angle relative to the thrust axis $\cos\psi = |(\hat{\mathbf{n}} \cdot \mathbf{P}_h)|/|\mathbf{P}_h| > 0.8$ selects only tracks that have at least a certain fraction of their momentum along the thrust axis. After these selection criteria, the total data sample contains 711×10^6 $\pi^+\pi^-$ pairs (1.58 di-pion pairs per event). Throughout this paper the order of the pion pairs used for calculating $\mathbf{R}_{1,2}$ is always $\pi^+\pi^-$ in both hemispheres. The data is binned in either 8×8 m_1, m_2 bins between 0.25 GeV/c^2 and 2 GeV/c^2 or in 9×9 z_1, z_2 bins between 0.2 and 1.0. The first method of assessing the interference fragmentation function is based on measuring a $\cos(\phi_1 + \phi_2)$ modulation of two hadron pair yields ($N(\phi_1 + \phi_2)$) on top of the flat distribution due to the unpolarized part of the fragmentation functions. The unpolarized part is given by the average bin content $\langle N_{12} \rangle$. The normalized distribution is then defined as $R_{12} := \frac{N(\phi_1 + \phi_2)}{\langle N_{12} \rangle}$. The two-pion pair yields $N(\phi_{1(R)} + \phi_{2(R)})$ are obtained for each kinematic bin in 16 equal-size bins of the azimuthal angles. The normalized azimuthal di-hadron yields, $R_{12(R)}$ can be parameterized as:

$$R_{12(R)} = a_{12(R)} \cos(\phi_{1(R)} + \phi_{2(R)}) + b_{12(R)} + c_{12(R)} \sin(\phi_{1(R)} + \phi_{2(R)}) + d_{12(R)} \cos 2(\phi_{1(R)} + \phi_{2(R)}) \quad (3)$$

where the parameter $b_{12(R)}$ should be unity due to the normalization. The parameter $a_{12(R)}$ is the amplitude proportional to the interference fragmentation functions. The normalized distribution is fit to equation (3) with $a_{12(R)}$, $b_{12(R)}$, $c_{12(R)}$ and $d_{12(R)}$ as free parameters. The reduced χ^2 values of the individual fits over all run ranges and bins are well described by a χ^2 distribution with a mean value close to unity.

The PYTHIA event generator used in this analysis does not contain the spin effects related to the IFF, and thus all asymmetries are expected to vanish. A check is performed for the kinematic effects that could mimic the spin-induced asymmetries. For this purpose light quark (uds) events and charm quark events have been generated, which were tracked through the detector in a GEANT simulation and then fully reconstructed. Asymmetries were evaluated at the generated 4-momentum level, as well as for reconstructed events. The results of this analysis are summarized in Table I, where effects of a finite detector acceptance are clearly visible. They can be significantly reduced via the opening angle selection. The sum of the absolute value of the reconstructed asymmetries and their statistical uncertainties in the simulated sample were assigned as bin-by-bin systematic uncertainties of the data asymmetries. They represent the largest systematic uncertainties, which are up to several % in the lowest statistics bins.

Mixed events: As the asymmetry requires a correlation between the hadron pairs on the quark and the anti-

TABLE I: MC results in % averaged over all z bins for generated uds events (uds gen), within the geometrical acceptance (uds gen. acc.) as well as reconstructed uds and charm events.

Sample	z_1, z_2-Asymmetries	
	$\langle a_{12} \rangle$	$\langle a_{12R} \rangle$
No opening angle cut		
uds gen.	-0.089 ± 0.008	-0.108 ± 0.008
uds gen. acc.	-0.488 ± 0.011	-0.490 ± 0.011
uds rec.	-0.401 ± 0.007	-0.428 ± 0.007
charm rec.	-0.446 ± 0.041	-0.388 ± 0.044
With opening angle cut of 0.8		
uds gen.	-0.038 ± 0.013	-0.035 ± 0.013
uds gen. acc.	-0.112 ± 0.016	-0.113 ± 0.016
uds rec.	0.020 ± 0.010	0.006 ± 0.010
charm rec.	0.006 ± 0.040	0.027 ± 0.040

quark side of an event, taking one hadron pair of another event should destroy this correlation and the asymmetries obtained for such a mixed-event data sample should vanish unless detector effects introduce artificial asymmetries. Two ways of extracting event-mixed asymmetries were applied: using a hadron pair of a first event in combination with a pair of a second event, and taking the axis information either from the first or the second event. The values from data are $(-0.019 \pm 0.017)\%$ for a_{12} and $(-0.012 \pm 0.017)\%$ for a_{12R}. These values are included as absolute systematic uncertainties in the results. Studies of polarization build-up in the KEK rings were performed earlier and were consistend with no beam polarization [3].

Higher harmonics: The higher-order terms in Eq. (3) are needed to reproduce the azimuthal variations well. Generally these different harmonics are orthogonal and should not interfere with each other, but a limited acceptance can introduce other asymmetries. The small differences in $a_{12(R)}$ of up to 1% between either fitting the first two terms or all are assigned as a bin-by-bin systematic uncertainty.

Weighted MC asymmetries: Artificial asymmetries were introduced into the MC generator for hadron pairs around the quark-antiquark axis and then reconstructed to test the validity of the reconstruction method. The a_{12} asymmetries, which depend directly on using the thrust axis as a proxy for the quark-antiquark axis, are reconstructed to $(92 \pm 1)\%$ of the generated value, and the a_{12R} asymmetries to $(99 \pm 1)\%$. Corresponding correction factors are applied to the measured asymmetries and the uncertainties were assigned as a systematic error.

Process contributions: The thrust selection alone already reduces the background from $\Upsilon(4S)$ decays to a negligible level. The charm contribution, however, has nearly the same thrust distribution as that for light quarks. On the other hand, since pions from charmed mesons are the product of a decay chain, the fractional energies fall off more rapidly than for light quarks. There-

fore the relative charm contribution also falls off from nearly 50% at lowest z bins to a few % at high z. The charm contribution in the mass bins first falls as can be seen in Fig. 2 but then increases again for invariant masses around 1 GeV/c^2.
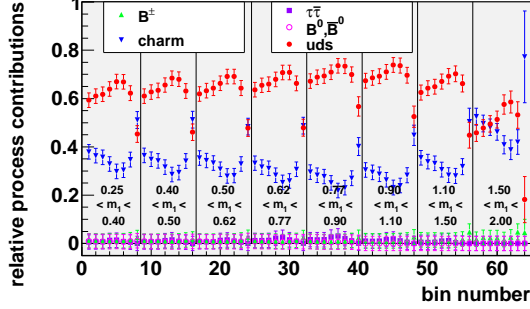

FIG. 2: Relative contributions of various processes for pion pairs as a function of the 8×8 m_1, m_2 bin number. The closed circles denote light quark-antiquark pair events, inverted triangles – charm events, triangles – charged B meson pairs, open circles – neutral B meson pairs and squares – τ pairs.

There is a small contribution from τ pairs rising to several % at high z. When analyzing a τ enhanced data sample without the minimal energy requirement one finds asymmetries of $a_{12} = (-1.31 \pm 0.13)\%$ averaged over the whole kinematic range. This asymmetry can be explained by the sizeable residual contribution from continuum events in the τ enhanced data. The relative contributions from τ pair events multiplied by their average asymmetry are added as systematic error, which is, however, negligibly small.

Correlation studies: In order to exclude possible effects of correlations between different kinematic and azimuthal bins, MC studies have been performed, which did not find any such effects.

Inverted thrust selection: The inverse thrust selection was also analyzed to test whether the azimuthal correlation of the two hadron pairs decreases. On average the asymmetries were 45% smaller.

Results: The results can be seen in Fig. 3 as a function of the fractional energies and in Fig. 4 as a function of the di-pion invariant masses. One sees large asymmetries monotonically decreasing with fractional energy and invariant mass with an indication of leveling off at the highest invariant masses. At higher masses or fractional energies an asymmetry of up to 10% corresponds to interference fragmentation functions of more than 30% the size of the corresponding unpolarized two-hadron fragmentation function. The results averaged over all kinematic bins are summarized in Table II. The a_{12R} results show similar dependencies and magnitudes. All results, their central values and process fractions are tabulated in the electronic supplement to this publication [29].
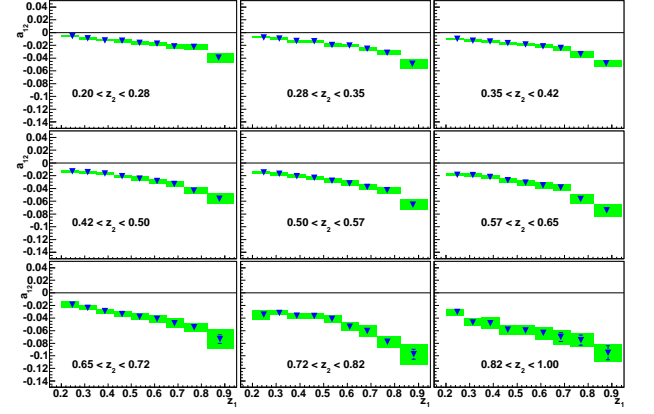

FIG. 3: a_{12} modulations for the 9×9 z_1, z_2 binning as a function of z_1 for the z_2 bins. The shaded (green) areas correspond to the systematic uncertainties.
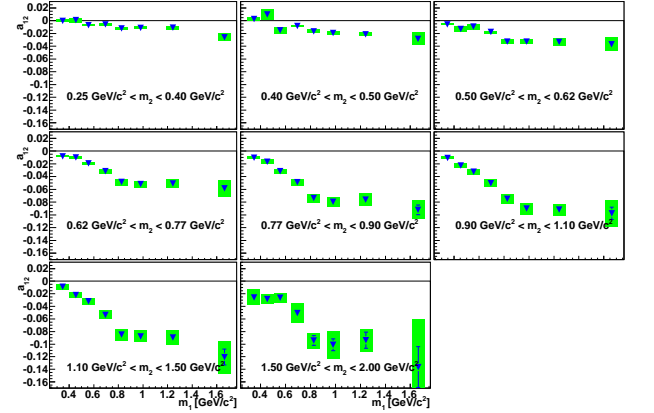

FIG. 4: a_{12} modulations for the 8×8 m_1, m_2 binning as a function of m_2 for the m_1 bins. The shaded (green) areas correspond to the systematic uncertainties.

Summary: Large azimuthal asymmetries for two $\pi^+\pi^-$ pairs in opposite hemispheres were extracted from a 672 fb^{-1} data sample. The asymmetries monotonically decrease as a function of $z_{1,2}$ and $m_{1,2}$ and no sign change is observed in contrast to [18]. The interference fragmentation function can be extracted from those asymmetries and used in a global fit to the SIDIS data [9, 10] to obtain the transversity distribution function.

TABLE II: Integrated asymmetries for the two reconstruction methods and their average kinematics.

$\langle z_1 \rangle, \langle z_2 \rangle$	0.4313
$\langle m_1 \rangle, \langle m_2 \rangle$	0.6186 GeV/c^2
$\langle \sin^2 \theta_t / (1 + \cos^2 \theta_t) \rangle$	0.7636
$\langle \sin \theta_{1d} \rangle, \langle \sin \theta_{2d} \rangle$	0.9246
$\langle \cos \theta_{1d} \rangle, \langle \cos \theta_{2d} \rangle$	0.0013
a_{12}	$-0.0196 \pm 0.0002(stat.) \pm 0.0022(syst.)$
a_{12R}	$-0.0179 \pm 0.0002(stat.) \pm 0.0021(syst.)$

[1] J. C. Collins, S. F. Heppelmann and G. A. Ladinsky, Nucl. Phys. B **420**, 565 (1994).
[2] R. Seidl *et al.* [Belle Collaboration], Phys. Rev. Lett. **96**, 232002 (2006).
[3] R. Seidl *et al.* [Belle Collaboration], Phys. Rev. D **78**, 032011 (2008).
[4] M. Anselmino, M. Boglione, U. D'Alesio, A. Kotzinian, F. Murgia, A. Prokudin and C. Turk, Phys. Rev. D **75**, 054032 (2007).
[5] A. Airapetian *et al.* [HERMES Collaboration], Phys. Rev. Lett. **94**, 012002 (2005).
[6] V. Y. Alexakhin *et al.* [COMPASS Collaboration], Phys. Rev. Lett. **94**, 202002 (2005).
[7] M. Gockeler *et al.* [QCDSF Collaboration], Nucl. Phys. A **755**, 537 (2005).
[8] F. A. Ceccopieri, M. Radici and A. Bacchetta, Phys. Lett. B **650**, 81 (2007).
[9] A. Airapetian *et al.* [HERMES Collaboration], JHEP **0806**, 017 (2008).
[10] H. Wollny [COMPASS Collaboration], arXiv:0907.0961 [hep-ex].
[11] R. Yang [PHENIX Collaboration], AIP. Conf. Proc. 1182 (2009).
[12] X. Artru and J. C. Collins, Z. Phys. C **69**, 277 (1996).
[13] D. Boer, R. Jakob and M. Radici, Phys. Rev. D **67**, 094003 (2003).
[14] J. C. Collins and G. A. Ladinsky, PSU-TH-114, 18 (1994).
[15] A. Bacchetta and M. Radici, Phys. Rev. D **67**, 094002 (2003).
[16] M. Radici, R. Jakob and A. Bianconi, Phys. Rev. D **65**, 074031 (2002).
[17] A. Bianconi, S. Boffi, R. Jakob and M. Radici, Phys. Rev. D **62**, 034008 (2000).
[18] R. L. Jaffe, X. Jin and J. Tang, Phys. Rev. Lett. **80**, 1166 (1998).
[19] A. Bianconi *et al.*, Phys. Rev. D **62**, 034009 (2000).
[20] A. Bacchetta and M. Radici, Phys. Rev. D **74**, 114007 (2006).
[21] A. Bacchetta, F. A. Ceccopieri, A. Mukherjee and M. Radici, Phys. Rev. D **79**, 034029 (2009).
[22] P. Estabrooks and A. D. Martin, Nucl. Phys. B **79**, 301 (1974).
[23] S. Kurokawa and E. Kikutani, Nucl. Instr. and Meth. A **499**, 1 (2003), and other papers included in this volume.
[24] A. Abashian *et al.* (Belle Collab.), Nucl. Instr. and Meth. A **479**, 117 (2002).
[25] Z. Natkaniec *et al.* (Belle SVD2 Group), Nucl. Instr. and Meth. A **560**, 1 (2006).
[26] E. Nakano *et al.*, Nucl. Instr. and Meth. A **494**, 402 (2002).
[27] T. Sjöstrand, L. Lonnblad, S. Mrenna, and P. Skands, PYTHIA 6.3 physics and manual, hep-ph/0308153, (2003).
[28] R. Brun, F. Bruyant, M. Maire, A. C. McPherson and P. Zanarini, CERN-DD/EE/84-1 (1984).
[29] electronic supplement file to this publication, available online.